Development of a planar dynamics model for vehicles

Matheus Henrique Rodrigues Miranda
Ludmila C. A. Silva
Jony J. Eckert
Maria Augusta M. Lourenço
Fabrício L. Silva
Franco G. Dedini
University of Campinas (UNICAMP)

ABSTRACT

Vehicle dynamics analyze the interactions among the vehicle, environment and driving style/profile applied. The tires are one of the most important components because all traction and braking forces are acting directly in the contact between the tire and ground. Therefore, this work focuses on the study of nonlinear Pacejka tire model, known as Magic Formula. The Pacejka equations are extensively applied in vehicle planar dynamics simulations. First, a vast bibliography review was performed aiming at the available tire models, considering its effects in the vehicle longitudinal and lateral dynamics. This paper presents the method to calculate the forces/efforts in planar behavior, necessary to determine torque, speed, power and others factors that can be used to design the vehicle control. The selected mathematical model was then implemented in Matlab/Simulink® environment, which enables an analysis of the slip and the tire forces according to the performed maneuvers. Finally, the resulting forces and vehicle dynamic response are compared, according to the variations of Pacejka parameters.

Keywords: Vehicle dynamics. Magic Formula. Tire.

INTRODUCTION

In recent years, relevant research has been carried out to improve driving safety and reducing accidents. Consequently, attention has been given to the development the stability and steerability control systems such as Electronic Stability Control (ESC), different active steering, and active braking control systems [1]. The ESC systems prevent the vehicle from losing control in risky situations, such as slippery floors and sudden deviations of the route. The ESC has sensors that monitor the speed of each wheel, and the overall yaw rate of the vehicle. When these sensors detect that the vehicle is not following the direction indicated by the steering wheel position, ESC applies the brakes to the individual wheels to provide stability and help the driver stay on course. For example, if the system detects that the rear wheels have started to slide to the right and the vehicle is turning counterclockwise, it can activate the brake to the right front wheel, generating a clockwise rotation to neutralize the yaw and stabilize the vehicle [2]. However, this system requires a vehicle dynamics model that accurately describes its behavior under different driving conditions.

The main features that affect the performance of the vehicle and, therefore, require greater power are the longitudinal and lateral dynamics. To determine the vehicle's performance in acceleration, braking, and turning, it is necessary to understand its longitudinal and lateral behavior. The longitudinal dynamics describes the transfer of masses between the front and rear axles due to the acceleration or braking movement of the vehicle, during travel, it is subjected to many resistance forces, such as rolling, climbing, aerodynamic and inertial resistance. [3]. Lateral dynamics studies the behavior of the vehicle in maneuvering and changing the direction of movement. Therefore, this reaction causes a lateral transfer of load from the internal tires in relation to the curve to the external tires. The tire cornering force keeps the vehicle in the corner and stabilizes the vehicle's movement [2].

The tire is the component of the vehicle responsible for the contact with the ground, therefore, estimating the tire-road contact forces is fundamental to describe the vehicle's dynamic behavior. Tire forces have nonlinear and complex relations with quantities associated with the tire such as physical properties and geometric measures, temperature, tire pressure, longitudinal and lateral slips, and the contact surface. There are several models to determine the interaction between the tire and the ground, which include theoretical (or physically based), empirical, and semi-empirical models [3]. The importance of estimating the forces acting on the contact between the tire and the ground is reflected in the amount of work done in this field, as shown in Fig. 1.

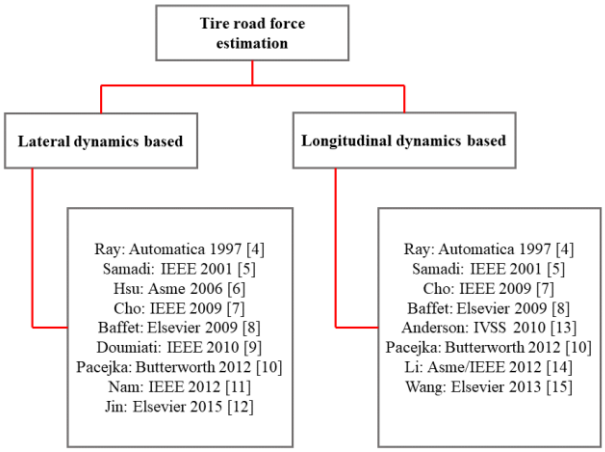

Figure 1. State-of-the-art literature review [16].

Among the several methods to estimate the tire forces, the semi-empirical Pacejka model, known as Magic Formula, is widely employed in the analysis and modeling of the vehicle dynamics. The formula contains several coefficients that are functions of the effective parameters. These parameters have physical meanings that are useful for the characterization of properties tire force production.

The Magic Formula can model accurately the tire force and moment data. Mashadi et al. [17] present a technique that relates the coefficients of the Magic Formula tire model to the physical properties of the tire using a finite element model. The Magic Formula coefficients are obtained from the validated model by using nonlinear least square curve fitting and genetic algorithm techniques. To identify the tire is force properties, the model output is compared with the available tire information. Rao et al. [18] identify the interactions among various tire design attributes and operating conditions, and the Magic Formula coefficients, through experimentation of tires using a simulation of finite element analysis. A detailed analysis is presented to discuss the influence of various design attributes and operating conditions on the Magic Formula parameters. Hüsemann et al. [19] discuss the impact of the difference in tire measurement results caused by using different test rigs and the effect of different measurement procedures on the tire modeling performance and vehicle dynamics output.

Arat et al. [20] examine such a method where a tire-attached sensor unit (intelligent tire system) provides tire slip ratio information, tire forces, tire slip angle, and also the potential performance improvements offered by integrating this system with an adaptive vehicle stability controller. Lee et al. [21] present a real-time maximum tire-road friction coefficient estimation method using the relationship between the wheel slip ratio and the friction coefficient. An effective tire radius observer and a tire normal force observer have been designed for the computation of the slip ratio from wheel speed and vehicle speed measurements. For the friction coefficient estimation, been used a tractive force estimator, a brake gain estimator, and a normal force observer. Singh [16] states that an integrated approach gives us the capability to reliably estimate friction for a wider range of excitations (both low-slip and high-slip conditions). Therefore, your work presents an integrated approach using an intelligent tire-based friction estimator and the brush tire model-based estimator. The of road friction information in the vehicle is used to apply in control systems from vehicle.

The objective of this work is to develop a planar model using the Magic Formula to describe the lateral and longitudinal forces acting between the tire and ground according to the maneuvers performed. To evaluate the influence of the Magic Formula coefficients on the vehicle behavior, changes were made considering two types of tire models, therefore it was possible to compare the vehicle behavior for both situations.

Aiming to achieve this purpose, this work is organized into the following sections: the tire models section, that presents the available models, considering its effects in the vehicle longitudinal and lateral dynamics; a section which describes the Magic Formula based on the version of 1987; a section that discusses the influence of its parameters in the shape of the forces curve; a section that discusses the difference caused by the variation of the parameters in the longitudinal solicitation of the vehicle to perform a certain driving cycle and a section that presents and discusses the difference caused by the variation of the parameters in the curve behavior vehicle considering two tire models. Finally, the main contributions of this work are summarized in the conclusion section.

TIRE MODELS

The dynamic tire models aim to describe their behavior by predicting the forces and moments acting at the tire contact interface with the ground. The levels of complexity and accuracy vary according to the category of the model chosen. Theoretical models include the physical structure of the tire, while empirical models make use of mathematical formulations to describe the characteristics based on experiments [10].

The Fig. 2 presents the tire model categories according to the developed approach. The models on the extreme left are based on experiments with full-scale tires. The models in the middle are simpler and less precise [10]. At models the far right the description becomes complex and less suitable for application in the simulation of vehicle motions, being more appropriate for the analysis of detailed tire performance in relation to the structure and physical behavior resulting from its deformation [22].

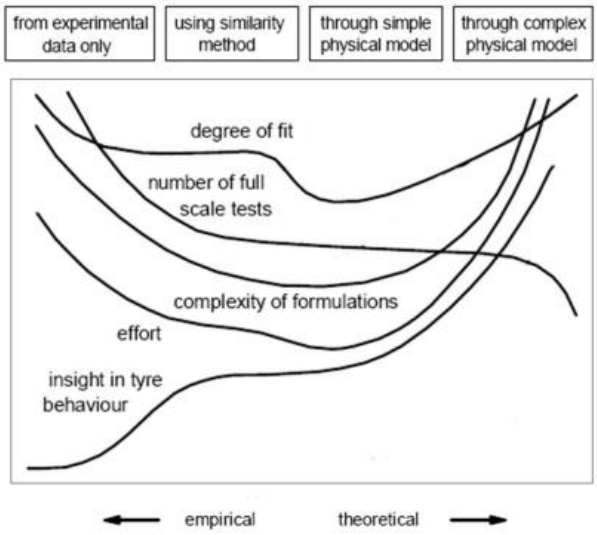

Figure 2. Tire model categories [10].

There are two categories of physical models. Firstly, complex theoretical physical models analyze the tire in detail using the finite element method and are commonly used in constructive analysis and in high-frequency excitations because it considers the effects arising from the deformation of the tire. These models can represent carcass deflection and be used to determine the total forces and moment through the tread elements motion and the integration of frictional forces.

As an example of the first category, the FTire, Flexible Ring Tire Model, a nonlinear model capable of simulating high frequencies and short wavelengths, and it is accurate in simulating the characteristics of tires in a steady-state, considering the internal damping and structural stiffness. The ring is numerically approximated by a finite number of belt elements, that are coupled with their direct neighbors by stiff springs and by bending stiffnesses [23]. Therefore, the degrees of freedom from the model describe the elements longitudinal rotation angle relative to the rim, and the elements bending in the lateral direction. The rotation angles are coupled by rotational stiffnesses, between two adjacent belt elements, as well as rotational stiffness for each belt element, located between the belt elements and rim. At the same time, the coupling between the lateral displacement of a belt element and its torsion angle is considered by an appropriate coupling stiffness [24].

The second category is simple physical models, describing the physical behavior of tires with simple analytical equations. One of the models in this category is the Tire Brush Model, which represents the tire as a series of bristles, these models simulate the elasticity and deformability due to the tire and ground interaction [24]. The pressure distribution and, hence, the maximum deflection vary according to a parabola curve. To pure side slip, the brush model moving at a constant slip angle develops a contact line which is straight and parallel to the velocity vector in the adhesion region and curved in the sliding region, where the available frictional force becomes lower than the force required so that the tips of the elements to follow the straight line, as shown in the Fig. 3. For this model, the deformation of the tread element at the leading edge is not considered [10].

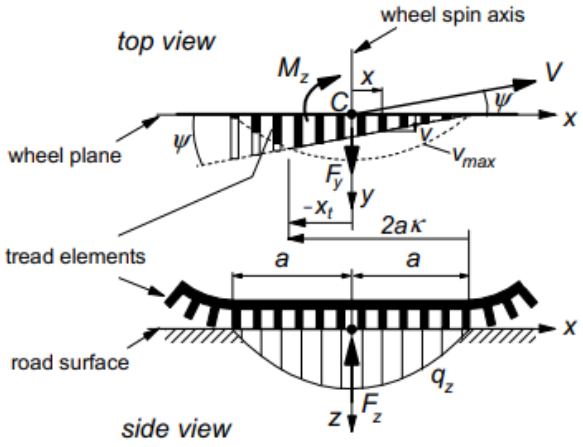

Figure 3. Top and side view from brush model moving at pure slip angle [10].

For the pure longitudinal slip, an imaginary point is attached to the wheel rim and is located, at the instant considered, a distance equal to the effective rolling radius r_e (defined at free rolling) below the wheel center as seen in Fig. 4 (at the instant considered). This point is known as the slip point (S). In free-rolling, by definition, the slip point S has zero velocity. Then, it forms the instantaneous center of rotation of the wheel rim. When the wheel is braked, point S moves forward with a positive longitudinal slip velocity (V_{Sx}). When it is driven, S point moves backward with consequently a negative slip speed [10].

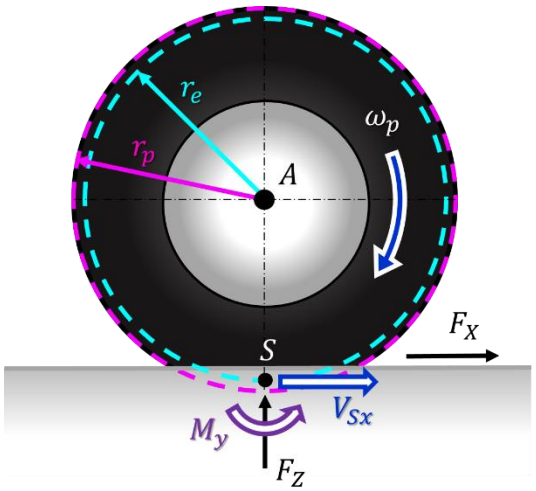

Figure 4. Tire features and movement indications [10].

The empirical models can be divides divided into two categories: empirical and semi-empirical. The empirical models are the tire models that describe the tire behavior using only mathematical formulas that fit real test data obtained in standardized tests on tire test benches, as shown by Santiciolli (2018) [22], Silva (2011) [25], and Mendonça (2019) [26]. The semi-empirical models can describe tire behavior through distortion and rescaling and by combining fundamental tire characteristics from measured data. They are also appropriate for real-time computations, despite being simple models and not very accurate [27]. An empirical model example is Magic Formula, presented initially by Pacejka and Bakker in 1987. This formula has several versions developed over the years and its coefficients and parameters change according to the model year considered, such as the models PAC87, PAC89, PAC94, and PAC2002 [10]. However, the equations described in this paper are taken from the 1987 version (PAC87).

MAGIC FORMULA TIRE MODEL PAC87

The Magic Formula tire model gives a relationship between the slip and the forces at different normal loads and inclination angles. The slip is the slip ratio in the case of longitudinal force and slip angles in the case of lateral force and self-aligning torque. The Magic Formula equation basic is present in Eq. 1 to Eq. 3 [28]:

$$y = D\,sin(C\,tan^{-1}\{B - E[B - tan^{-1}(B)]\}) \quad (1)$$

$$Y(x) = y(x) + S_v \quad (2)$$

$$x = X + S_h \quad (3)$$

where Y is the output variable that can be a longitudinal force (F_x), lateral force (F_y), or self-aligning torque (M_z), and X is the input variable that can be the slip angle (α) or the longitudinal slip (κ). The parameter B is stiffness factor, C the shape factor, D the peak factor, E the curvature factor, S_h the horizontal shift, and S_v the vertical shift.

The slip ratio longitudinal is a function from speed in the center of the wheel (V_x), rotational speed of the tire (ω_p), and effective radius of the wheel (r_e) and can be calculated by Eq. 4 [10]:

$$\kappa = -\frac{V_x - r_e\omega_p}{V_x} \quad (4)$$

The slip angle is a function of the lateral speed (V_y) and wheel speed, as shown in Eq. 5.

$$\alpha = tan^{-1}\left(-\frac{V_y}{V_x}\right) \quad (5)$$

The parameter D represents the peak value and the product BCD corresponds to the slope at the origin. The shape factor C controls the limits of the range of the sine function appearing in the formula and thus determines the shape of the resulting curve. The factor B is left to determine the slope at the origin. The factor E is introduced to control the curvature at the peak and, at the same time, the horizontal position of the peak [10].

An example from the Magic Formula tire model is shown in Fig. 5 that presents typical variations of the lateral force (F_y) versus the lateral slip angle (α).

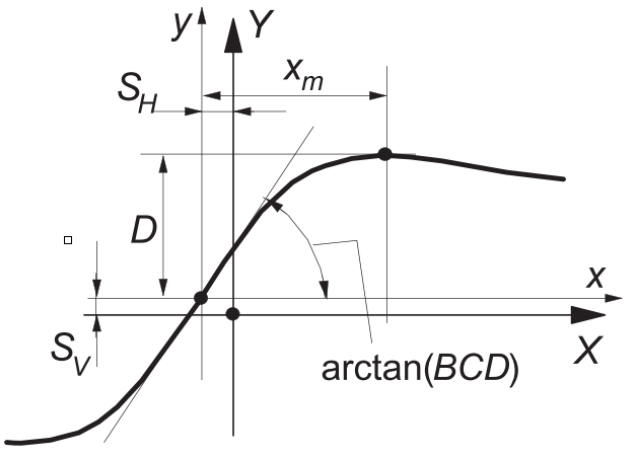

Figure 5. The tire lateral force and Magic Formula parameters [10].

These parameters are expressed in terms of secondary coefficients as shown in Eq. 6 to Eq. 25:

- Lateral force:

$$C = a_0 \quad (6)$$

$$D = \mu_{yp}F_z \quad (7)$$

$$\mu_{yp} = a_1F_z + a_2 \quad (8)$$

$$BCD = a_3\,sin[2\,tan^{-1}(F_z/a_4)]\,(1 - a_5|\gamma|) \quad (9)$$

$$E = a_6F_z + a_7 \quad (10)$$

$$S_h = a_8\gamma + a_9F_z + a_{10} \quad (11)$$

$$S_v = a_{11}\gamma F_z + a_{12}F_z + a_{13} \quad (12)$$

- Longitudinal force:

$$C = b_0 \quad (13)$$

$$D = \mu_{yp} F_z \quad (14)$$

$$\mu_{yp} = b_1 F_z + b_2 \quad (15)$$

$$BCD = (b_3 {F_z}^2 + b_4 F_z) e^{-b_5 F_z} \quad (16)$$

$$E = b_6 {F_z}^2 + b_7 F_z + b_8 \quad (17)$$

$$S_h = b_9 F_z + b_{10} \quad (18)$$

$$S_v = 0 \quad (19)$$

- Self-aligning torque:

$$C = c_0 \quad (20)$$

$$D = c_1 {F_z}^2 + c_2 F_z \quad (21)$$

$$BCD = (c_3 {F_z}^2 + c_4 F_z)(1 - c_6|\gamma|) e^{-c_5 F_z} \quad (22)$$

$$E = (c_7 {F_z}^2 + c_8 F_z + c_9)(1 - c_{10}|\gamma|) \quad (23)$$

$$S_h = c_{11}\gamma + c_{12} F_z + c_{13} \quad (24)$$

$$S_v = (c_{14} {F_z}^2 + c_{15} F_z)\gamma + c_{16} F_z + c_{17} \quad (25)$$

However, when it comes to a combined slip condition, the forces can be obtained by using the elliptical approximation [29], as is illustrated in Fig. 6.

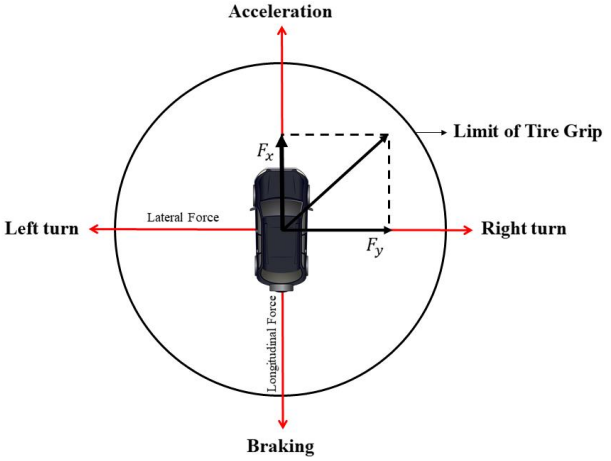

Figure 6. Friction circle of tire [16].

That approximation can be obtained using the Eq. 26.

$$\left(\frac{F_x}{F_{x_{max}}}\right)^2 + \left(\frac{F_y}{F_{y_{max}}}\right)^2 = 1 \quad (26)$$

where the force $F_{y_{max}}$ is exerted, at the given sideslip angle, when no force F_x is exerted, and $F_{x_{max}}$ is the maximum longitudinal force exerted at zero sideslip angle.

VEHICLE LONGITUDINAL DYNAMICS

To validate the torque required by the Magic Formula in a given driving cycle will be applied the dynamics methodology proposed by Gillespie [30] whose model is based on the resistance forces acting in the vehicle.

Rolling resistance results from an energy loss due to the tire deformation and adhesion in the contact area. At low speeds, the rolling resistance is the main resistance load. The rolling resistance is shown in Eq. 27.

$$R_x = mg\,(0.015 + 7\,x\,10^{-6}\,Vel^2) \quad (27)$$

where m is the vehicle mass (kg), g is the acceleration of gravity (m/s^2) and *Vel* is the vehicle speed (m/s).

The Eq. 28 defines the air resistance against the vehicle passage or aerodynamic drag.

$$D_A = \frac{1}{2}\,\rho\,C_d\,A_f\,Vel^2 \quad (28)$$

where ρ is the air density (kg/m^3), C_d is the drag coefficient, and A_f is the frontal area (m^2).

The simulated driving cycle will be NBR6601 that considers null of the road grade, therefore the resistance to climbing will be null.

The requested torque is shown in Eq. 29

$$T_{req} = r\left(m\,a_{cyc} + \frac{I_w\,a_{cyc}}{r^2} + R_x + D_A\right) \quad (29)$$

where r is the tire external radius of the tire (m), a_{cyc} is the acceleration required by cycle (m/s^2) and I_w is the wheels and tires inertia (kg.m^2).

The available traction force is defined by the Eq. 30 as a function of the torque in the axle, inertia of the wheels, and tires, the radius of the tire and the acceleration of the vehicle (a_x).

$$F_x = T_{axle} + \frac{I_w\, a_x}{r} \tag{30}$$

The vehicle acceleration is determined as a function of the vehicle mass, the traction force, and the resistance forces, as shown in Eq. 31.

$$a_x = \frac{\sum F_x - R_x - D_A}{m} \tag{31}$$

As the propulsion system considered is that of in-wheel motors coupled directly to the vehicle wheels, the requested torque has that to be splits between the axle the rear and front. But according to Gillespie [30], the available driving power and restricted by the tire traction. Therefore, the vehicle traction limit is modeled as proposed by Jazar [31] and is shown in Eq. 32 and Eq. 33.

$$T_{front} = \left(\frac{mgc}{2L} - \frac{mha_x}{2L}\right)\mu\, r \tag{32}$$

$$T_{rear} = \left(\frac{mgb}{2L} - \frac{mha_x}{2L}\right)\mu\, r \tag{33}$$

where L is the vehicle wheelbase (m), b is the longitudinal distance between the vehicle front axle and the gravity center (m), c is the longitudinal distance between the vehicle rear axle and the gravity center (m), and μ is the tire-ground coefficient of friction.

INFLUENCE OF PARAMETERS OF MAGIC FORMULA

Each parameter influences the shape of the curve and this influence can be demonstrated graphically. The parameter B describes the initial slope and the fall of the curve after its peak, and parameter D presents the peak of the curve. The shape parameter C determines the shape of the resulting curve. The parameter E is introduced to control the curvature at the peak. Therefore, the C and E parameters can be easily appreciated in the shape of the curves. The value from B and D are the same for all curves, varying only the C and E values [10]. The force curves for different configurations of Pacejka parameters (C, D, and E) are presented in Fig. 7, Fig. 8, Fig. 9 and Fig. 10.

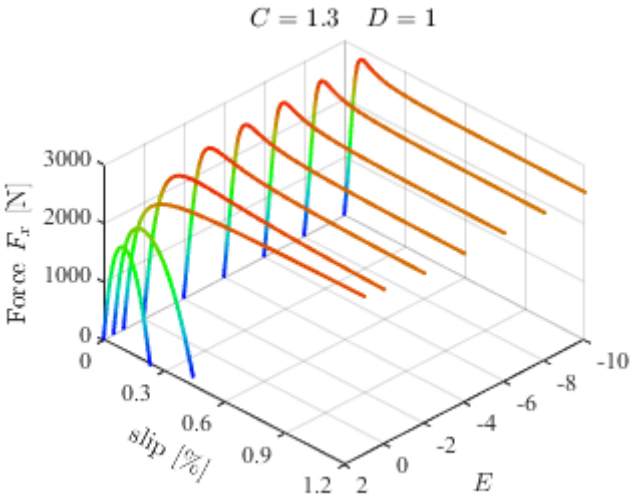

Figure 7. Influence of the curvature factor for a shape factor of 1.3 and peak factor of 1.

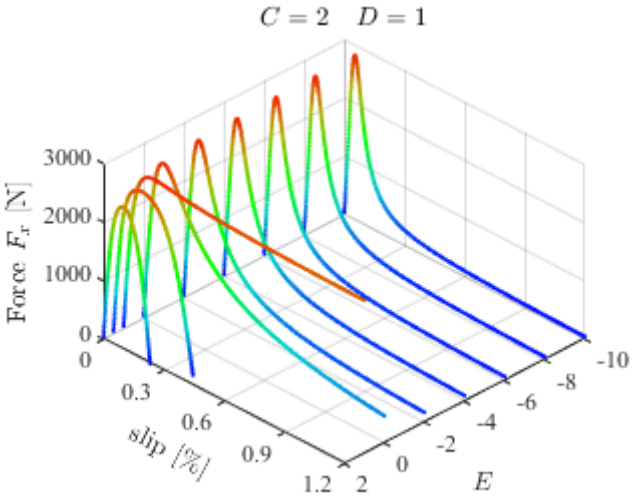

Figure 8. Influence of the curvature factor for a shape factor of 2 and peak factor of 1.

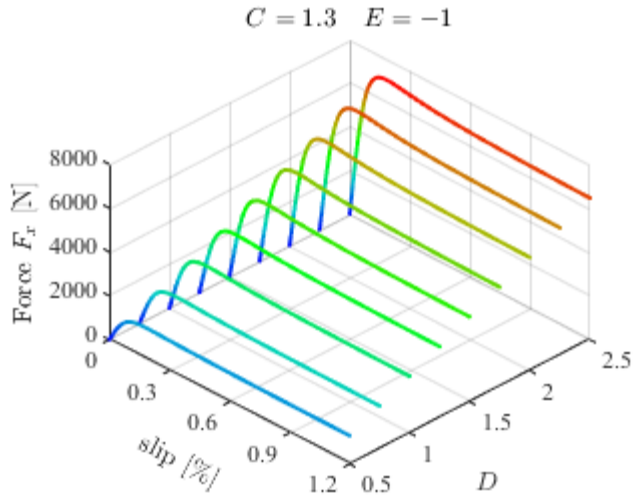

Figure 9. Influence of the peak factor for a shape factor of 1.3 and curvature factor of -1.

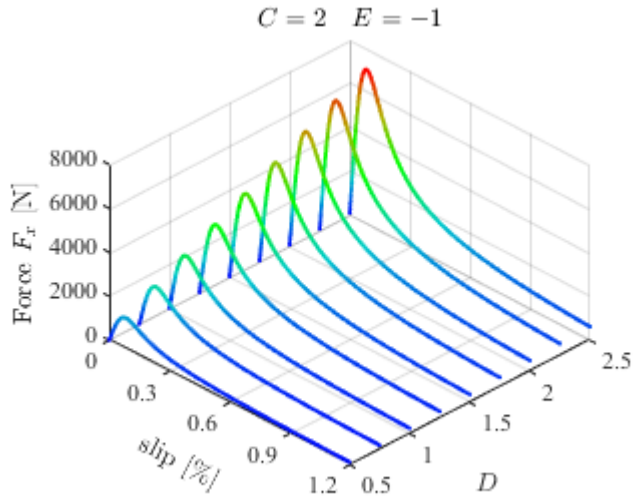

Figure 10. Influence of the peak factor for a shape factor of 2 and curvature factor of -1.

In Fig. 7 to 10, it is possible to analyze the influence of the shape factors C and E on the appearance of the curve. The influence of the shape parameter C easily can be observed in the figures, as bigger its value, as faster the part of the curve after the peak decreases.

Pacejka [10] notes that the value of curvature factor E when it is greater than 1, does not produce curves realistic. It can be observed also that values from –10 and -2 for parameter E does not change the curve shape as much as it does from -2 to 2, this can be very important for choosing the best curvature factor to fit the measured curves [13].

Therefore, these parameters can describe the vehicle handling. According to Rao [18], to have good vehicle control during emergency maneuvers, a high lateral force D is desirable. Although the combined effect of the coefficients of a_1 and a_2 decides peak value D, the influence of a_1 is dominant as this contains the term of normal load (F_z) and the variation of a_2 will be minimal for the same frictional conditions.

Tire cornering stiffness BCD is considered as the most influencing parameter for vehicle handling behavior [18]. Thus, an increase of a_3 and a_5 for the same a_4, or a reduction of a_4 for the same a_3 and a_5, between two tire options is a clear index of improved vehicle handling behavior.

According to Rao [18], the influence of self-aligning torque on steering forces is most significant with manual steering vehicles and is probably not so important for vehicles equipped with power steering. Variations in the parameters are not directly reflected in the Magic Formula coefficients because unlike the coefficients described in the lateral force, these have no physical meaning for the handling characteristics. Therefore, it can be concluded that they are only adjustment parameters. This is proven, because according to Rao [18] the coefficients c_3, c_4 and c_5 of BCD vary significantly for similar tires. The range of variation can be 10 times, with signal change.

To overcome the longitudinal peak friction, a higher peak value described by parameter D is desired for the longitudinal force. Similar to the lateral force, the parameter D is determined by the coefficients b_1 and b_2 that describe the contact friction. When reaching the limit conditions of traction, the wheels slip or lock due to the braking, which may cause the vehicle to lose control. To avoid this situation, anti-spin and anti-lock (ABS) devices are very important, because they avoid that the system works above the ideal curve.

When it comes to longitudinal force, the parameter B is also important as it determines the shape of the curve after the peak. Therefore, the higher its value, the part of the curve after the peak decreases faster. According to Rao [18], if the longitudinal force it is applied to the front axle it reduces the value of C and consequently makes the vehicle more understeering or less oversteering. The opposite effect is due to a longitudinal force applied to the rear axle.

VEHICLE PARAMETERS

The 1987 version of the Magic Formula was implemented in Matlab/Simulink®. The standard vehicle used in the simulations is based on by Genta [29], and the characteristics are shown in Tab. 1.

Table 1. Simulated vehicle parameters [29].

Parameters	
Mass	1150 kg
Wheelbase	2.660 m
Rear axle to gravity center	2.128 m
Front axle to gravity center	0.532 m
Gravity center height	0.570 m
Tire R13 radius	0.287 m
Tire R18 radius	0.310 m
Wheels and tires R13 inertia	2.4 kg.m^2
Wheels and tires R18 inertia	2.8 kg.m^2
Vehicle frontal area	2.06 m^2
Drag coefficient	0.36

LONGITUDINAL RESULTS

To evaluate the longitudinal dynamics the Brazilian urban driving cycle NBR6601 was used. The results obtained were compared with the methodology of the longitudinal dynamics evaluation proposed by Gillespie [30], as shown in Fig.11 where the vehicle with rim tire 13 was considered and Fig. 12 considering the rim tire 18. Its methodology is based on the sum of the forces acting on the vehicle in the direction of displacement.

The correlation coefficient was calculated to show the percentage of the variance between the methodologies, measuring the variability proportion between the two curves. This coefficient consists of the sum of the squares of the forecast errors obtained. It can be calculated through Eq. 34. The closer the value of R^2 to 1, the less variation between the variables.

$$R^2 = \frac{(\sum(x_i - \bar{x})\,(y_i - \bar{y}))^2}{\sum(x_i - \bar{x})^2\ \sum(y_i - \bar{y})^2} \qquad (34)$$

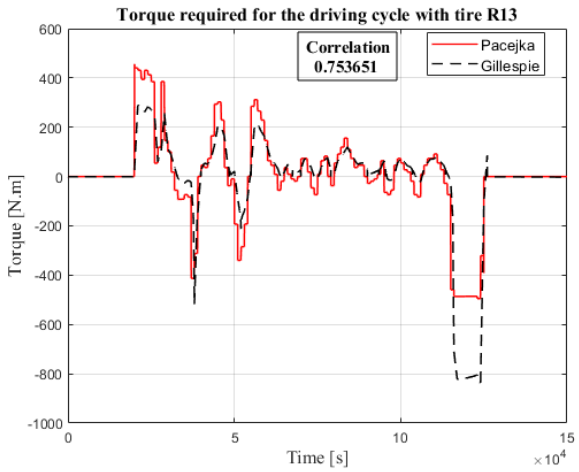

Figure 11. Torque required by Pacejka and Gillespie methodology for the driving cycle NBR6601 considering an R13 rim tire.

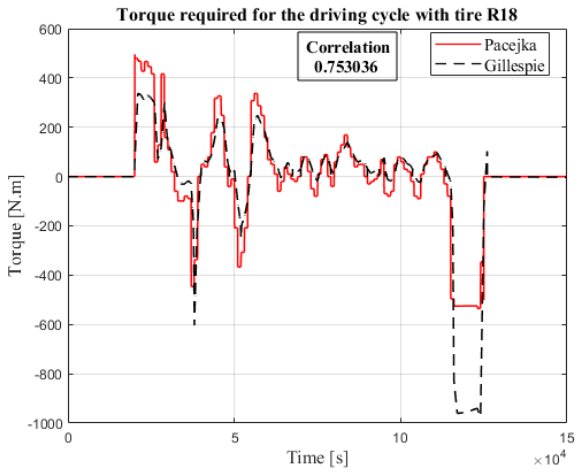

Figure 12. Torque required by Pacejka and Gillespie methodology for the driving cycle NBR6601 considering an R18 rim tire.

It can be observed that initially, the methodology of the Magic Formula requires a greater torque than Gillespie [30], this can be attributed to the fact that the formulation has greater precision to determine the longitudinal slip.

Although the correlation is not so high, it presents satisfactory values, considering the differences between the methodologies. But note that the trend of the curves is similar throughout the whole cycle. During the whole simulation, the torque required by the Magic Formula methodology is slightly higher than that required by Gillespie [30]. However, at times of great reduction in cycle speed, Gillespie [30] has higher values than the Magic Formula.

Comparing the cycle of the vehicle with rim tire 13 with the vehicle using rim tire 18, it is possible to observe that the required torque is higher for the rim 18 mainly at the beginning of the cycle. This occurs because the rim tire 13 presents less rolling resistance because it has a smaller width, since the tire if deforms in the contact area with the ground. This deformation causes the plies of the carcass to move by shearing the rubber and the tread is also deformed and stay subject to mechanical stress. These deformations generate energy consumption. Therefore, the smaller the contact area, the less energy is dissipated, which is why the rim tire 13 is less resistant.

LATERAL RESULTS

To evaluate the difference caused by the variation of the parameters at curve behavior vehicle, a constant radius maneuver with a wheel steering amplitude of 6 radians, a longitudinal speed of 20 m/s, and time of the simulation of 20 seconds was simulated. For all simulations the same vehicle characteristics were maintained, changing only the tire characteristics. The simulations were made considering an R13 rim tire and an R18 rim tire. All the coefficients of the Magic Formula were obtained in the work of the Genta [29].

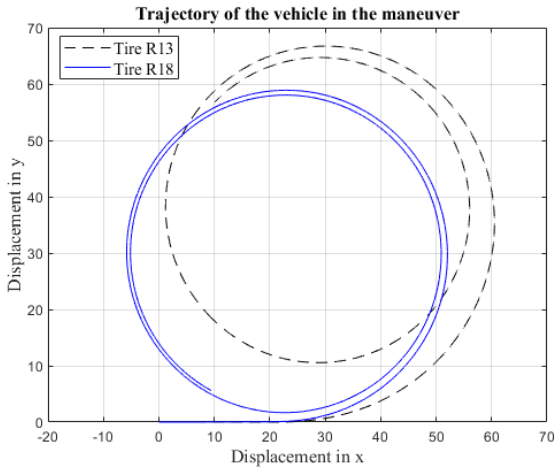

Figure 13. Trajectory of the vehicle considering an R13 rim tire and an R18 rim tire.

The tires, due to their flexibility slip in relation to the ground when performing the transmission of force. This transmission of forces depends on the friction available on contact, also called grip. The grip can be attributed, mainly, to the contact of the rubber with the ground. The rim tire 13 presents a greater slip to perform the maneuver when compared with the tire with rim 18, because it has a larger contact area, which provides a greater grip, ensuring greater stability in making the curve.

Another way to see this greater stability is by observing the Magic Formula coefficients. The D parameter shows the highest value of lateral force, as higher this value, as more control the vehicle will have in performing the maneuver. In Fig. 14 it is possible to observe the difference between the values of parameter D for the two tires when making the curve.

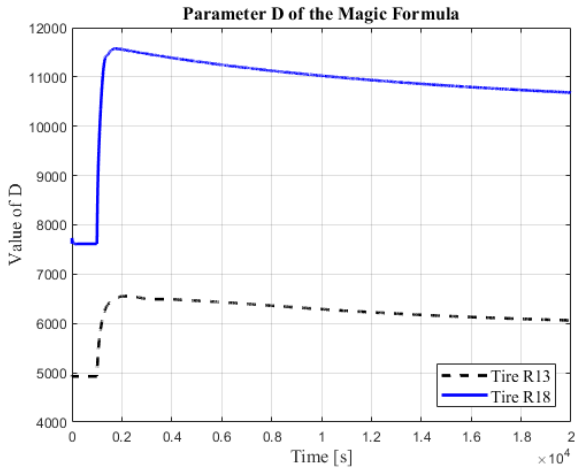

Figure 14. Peak factor in the tires for the maneuver.

The values of the coefficients a_1 to a_4 for lateral force have physical meaning [18]. The coefficient a_1 is the dependence on lateral friction, a_2 is the lateral friction level, a_3 is the maximum stiffness in the curves, and a_4 is the normal load in the maximum stiffness curve. It is possible to observe in Tab. 2 the difference between the values of these coefficients for the two types of tires. It is observed that the coefficient a_3, as being the maximum stiffness in the curves that the tire presents, has a greater value for the tire R18, having greater stability in the maneuver.

Table 2. Coefficients value.

Tire / Coefficient	**R13**	**R18**
a_1	- 34	0
a_2	1250	1688
a_3	3036	4140
a_4	12.80	6.0260

Although the combined effects of a_1 and a_2 decide the peak value of D, as a_1 multiplies the term squared of normal force, it is dominant. Therefore, by analyzing the values of a1 for the two types of tires, it is possible to see that the parameter D for tire R13 has a lower peak due to the value of a_1 being negative, and lower in comparison to tire R18.

CONCLUSION

The vehicle model was developed in order to initiate a future project in vehicle stability control. The implemented model, using PAC87, was validated based in some maneuver and driving cycle in Matlab/Simulink® software.

The model of the contact between wheel and ground was satisfactory, showing the behavior of the vehicle in longitudinal and lateral. From the result, it can be noticed the Pacejka model present similar behavior with Gillespie and also show the influence of the tire type in the vehicle trajectory. The model concept is already known and with this article was possible to visualize the implementation of the Pacejka model.

Another important point in this paper, it is all parameters in the Pacejka formula should be raised or calculated according to the specific vehicle position and condition, because they have direct influence in the vehicle behavior.

ACKNOWLEDGEMENTS

This work was conducted during scholarships supported by the Brazilian Federal Agency for Support and Evaluation of Graduate Education (CAPES) and the University of Campinas (UNICAMP).

REFERENCES

[1] LIE, A.; TINGVALL, C.; KRAFT, M.; KULLGREN, A. The Effectiveness of Electronic Stability Control (ESC) in Reducing Real Life Crashes and Injuries. Traffic Injury Prevention, 7:1, p. 38-43, 2006.

[2] DANG, J. N. Preliminary results analyzing the effectiveness of electronic stability control (ESC) systems. U.S. Department of Transportation, Washington, DC, 2004.

[3] RILL, G. Road Vehicle Dynamics: Fundamentals and Modeling. Boca Raton: CRC PRESS, 2012.

[4] RAY, L.R. Nonlinear tire force estimation and road friction identification: Simulation and experiments. Automatica, 33(10), p. 1819-1833, 1997.

[5] SAMADI, B.; KAZEMI, R.; NIKRAVESH, K. Y.; KABGANIAN, M. Real-time estimation of vehicle state and tire-road friction forces. Proceedings of the 2001 American Control Conference. IEEE, vol. 5, 2001.

[6] HSU, Y. H. J.; LAWS, S.; GADDA, C.D.; GERDES, J.C. A method to estimate the friction coefficient and tire slip angle using steering torque. ASME International Mechanical Engineering Congress and Exposition, vol. 47683, p. 515-524, 2006.

[7] CHO, W.; YOON, J.; YIM, S.; KOO, B.; YI, K. Estimation of tire forces for application to vehicle stability control. IEEE Transactions on Vehicular Technology, 59(2), p. 638-649, 2009.

[8] BAFFET, G.; CHARARA, A.; LECHNER, D. Estimation of vehicle sideslip, tire force and wheel cornering stiffness. Control Engineering Practice, 17(11), p. 1255-1264, 2009.

[9] DOUMIATI, M.; VICTORINO, A.C.; CHARARA, A.; LECHNER, D. Onboard real-time estimation of vehicle lateral tire–road forces and sideslip angle. IEEE/ASME Transactions on Mechatronics, 16(4), p. 601-614, 2010.

[10] PACEJKA, H.B. Tire and Vehicle Dynamics. 3rd ed. Butterworth-Heinemann, 2012.

[11] NAM, K.; FUJIMOTO, H.; HORI, Y. Lateral stability control of in-wheel-motor-driven electric vehicles based on sideslip angle estimation using lateral tire force sensors. IEEE Transactions on Vehicular Technology, 61(5), p. 1972-1985, 2012.

[12] JIN, X.; YIN, G. Estimation of lateral tire–road forces and sideslip angle for electric vehicles using interacting multiple model filter approach. Journal of the Franklin Institute, 352(2), p. 686-707, 2015.

[13] ANDERSSON, M.; BRUZELIUS, F.; CASSELGREN, J.; HJORT, M.; LÖFVING, S.; OLSSON, G.; YNGVE, S. Road friction estimation, Part II. IVSS project report, 2010.

[14] LI, L.; FEI-YUE, W.; QUNZHI, Z. Integrated longitudinal and lateral tire/road friction modeling and monitoring for vehicle motion control. IEEE Transactions on Intelligent Transportation Systems, vol. 7, p. 1–19, 2006.

[15] WANG, R.; WANG, J. Tire–road friction coefficient and tire cornering stiffness estimation based on longitudinal tire force difference generation. Control Engineering Practice, vol. 21, p. 65-75, 2013.

[16] SINGH, K. B.; TAHERI, S. Estimation of tire–road friction coefficient and its application in chassis control systems, Systems Science & Control Engineering, 3:1, p. 39-61, 2015.

[17] MASHADI, B.; MOUSAVI, H.; MONTAZERI, M. Obtaining relations between the Magic Formula coefficients and tire physical properties. International Journal of Automotive Engineering, vol. 5, 2015.

[18] RAO, K. N.; KUMAR, R. K.; MUKHOPADHYAY, R.; MISRA, R. A study of the relationship between Magic Formula coefficients and tyre design attributes through finite

element analysis. Vehicle System Dynamics, vol. 44, p. 33 – 63, 2006.

[19] HÜSEMANN, T.; WÖHRMANN, M. The impact of tire measurement data on tire modelling and vehicle dynamics analysis. Tire Sci Technol, vol. 38, p. 155–180, 2010.

[20] ARAT, M. A.; SINGH, K. B.; TAHERI, S. (2014). An intelligent tire based adaptive vehicle stability controller. International Journal of Vehicle Design, 65(2/3), 118–143.

[21] LEE, C.; HEDRICK, K.; YI, K. Real-time slip-based estimation of maximum tire-road friction coefficient. IEEE/ASME Transactions on Mechatronics, vol. 9, no. 2, p. 454-458, 2004.

[22] SANTICIOLLI, F. M. Parameterization of Tire Models applied to Small Tires. 2018. 151p. Thesis (Doctorate) - University of Campinas, Campinas, 2018 (in Portuguese).

[23] GIPSER, M. H. R.; LUNGNER, P. Dynamical Tire Forces Response to Road Unevennesses. Proceeding of 2nd Colloquium on Tire Models for Vehicle Analysis, 1997.

[24] FTire - Flexible Structure Tire Model Modelization and Parameter Specification. Cosin Scientific Software. Germany, 2020.

[25] SILVA, L. C. A. Identification and simulations of tire behavior aimed at implementing control in motorized wheelchairs. 2011. 153p. Thesis (Doctorate) - University of Campinas, Campinas, 2011 (in Portuguese).

[26] MENDONÇA, D. A.; SANTICIOLLI, F. M.; SILVA, L. C. A.; ECKERT, J. J.; DEDINI, F. G. Parameterization of Tire Model for Light Weight Vehicle Regarding the Combined Slip. International Congress of Mechanical Engineering, 25., 2019, Uberlândia.

[27] CASTELLVÍ, M. C. Benchmark of tyre models for mechatronic application. 2011. 91f. Master's Dissertation. University of Cranfield, Cranfield, 2011.

[28] BAKKER, E.; PACEJKA, H.B.et al. A new tire model with an application in vehicle dynamics studies. 4th Auto technologies Conference, Monte Carlo. SAE 890087, p.83-95, 1989.

[29] GENTA, G. Motor Vehicle Dynamics: Modeling and Simulation. Vol. 43. World Scientific. 1997.

[30] GILLESPIE, T. D. Fundamentals of vehicle dynamics. Society of Automotive Engineers – SAE, Warrendale, PA, USA, 1992.

[31] JAZAR, R. N. Vehicle dynamics: Theory and applications. Springer Science+ Business Media, New York, NY, USA: Springer, 2008.